Journal of Fluorescence (2018) 28:839–854
https://doi.org/10.1007/s10895-018-2249-9

ORIGINAL ARTICLE

Solvent Dependence on Structure and Electronic Properties of 7-(Diethylamino) - 2H -1- Benzopyran-2- one (C-466) Laser Dye

C. G. Renuka[1] · Y. F. Nadaf[2] · G. Sriprakash[2] · S. Rajendra Prasad[3]

Received: 30 March 2018 / Accepted: 7 June 2018 / Published online: 16 June 2018
© Springer Science+Business Media, LLC, part of Springer Nature 2018

Abstract

In this work, we studied influences on the absorption and fluorescence emission spectra of coumarin-4066 (C-466) with different solvent polarity scale. The spectral shifts reflect the effect of the equilibrium solvents association across the energized solute particle, which adjusts inertially as a result of quick charge realignment upon radiative deactivation to the lowest electronic state. The dipole moments of C-466 are determined by employing the Bakhshiev, Kawski-Chamma-Viallet, Lippert-Mataga and McRae relations. The results from all these methods are, excited state dipole moment of C-466 is higher than the ground state dipole moments and which indicates molecule is less polar in the ground state. Theoretical analysis was also carried out by Density Functional theory (DFT and TD –DFT) employing the BECKE-1998 (exchange)/STO-6G basic set in ethanol solvent and in vacuum medium. The HOMO-LUMO, Solvent Accessible Surfaces (SAS) and Molecular Electrostatic Potential (MEP) were analysed to acquire additional knowledge of the molecular arrangement and electronic properties of C-466. These photophysical properties suggest delineation can be mauled for laying out new luminescent tests for various solvents microenvironment.

Keywords Solvatochromism · Polarity functions · DFT and TD-DFT analysis · SAS · MEP · OLED

Introduction

The environment and energy of organic dye molecules in electronically excited conditions decide its photophysical and photochemical properties. In significant estimations the particle is expected verifiably towards disengaged, as though it stayed in the gaseous form at low density. In all actuality, we are apprehensive about particles in dense stage, fluids, gooey fluids and solids; the impact of these phases on the total and comparative energies of electronic conditions of solute molecular properties. In this manner the excited state solute molecule significantly changes in photochemistry and photophysics process. The photophysics properties of fluorescent dye has been playing a field of continuous attention since for improved considerate of the excited state molecular properties help not only in designing novel molecules but similarly in improving the performance of these as laser dyes, probes for polymers [1], micellar and in biological systems [2], molecular devices, photovoltaic cells [3], in dielectric enrichment [4], etc. The photophysical properties of coumarin dyes are a dynamic field of exploration for their prominence as laser materials. Maximum of the coumarins are extremely fluorescent and are widely used as laser dyes in blue-green wavelength region. The resilient fluorescence emission of coumarin molecules outcomes as of the polar atmosphere of their low lying excited states. This is known statistic that, the electronic spectra of these dyes are subjective by their direct medium. Amongst the foremost environmental aspects that influence the electronic spectrum, the effect of solvents is one of specific significance. A variation of solvent is usually convoyed by a change in dielectric parameter, polarity and polarizability of the medium. Therefore, changing the solvent distresses the excited state and the ground state properties [5, 6].

✉ Y. F. Nadaf
dryfnadaf@gmail.com

[1] Department of Physics, Bangalore University, Jnanabharathi Campus, Bengaluru 560056, India

[2] Department of Physics and Research Center, Maharani Science College for Women, Bengaluru 560001, India

[3] Department of Chemistry, University of Mysore, Mysuru 570005, India

Dipole moments are also used for determining the place of substitutional groups in aromatic compounds. Dipole moments of a molecule in the excited state is an another parameter that delivers important findings about the geometrical and electronic configuration of the molecule structure in the short-term excited state. Hence electric dipole moments of organic dye molecules have been broadly considered. Attentiveness of these molecule properties is persuaded by the rapid advancement in material research and for novel organic dye molecules in nonlinear ophthalmic nature. Outsized number of dyes are selected in many physical and chemical research laboratories intended for infrequent ophthalmic properties with higher excited state dipole moments. Dyes are used routinely in laser research [7] and medical applications, etc. [8], because of these quick advancements in photochemistry investigations of electric dipole moments in energized states acquired more significance. The various methods are used for obtaining the excited state dipole moments i.e., electro-optical methods (Stark splitting of 0–0 vibrational bands, electrochromism of absorption and fluorescence bands, fluorescence anisotropy in an external electric field) and the naivest, utmost extensively used by researchers are solvent shift method [9, 10].

This work reveals the study of the absorption and fluorescence spectra of Coumarin 466 (C-466), at room temperature in various solvents and subsequently the estimation of the dipole moment of the excited state (S_1) through the solvatochromic analysis of the data in accordance with Bakhshiev, Kawski-Chamma-Viallet, McRae and Lippert-Mataga relations. The HOMO-LUMO and MEP were also investigated using theoretical calculations [11, 12].

Materials and Methods

Materials

The laser dye (Coumarin 466) 7-(diethylamino) - 2H -1-benzopyran-2- one is procured from Exciton Company USA, have been used without other purification (purity 99%). Optimised structure of (Coumarin 466) C-466 is shown in Fig. 1. In this present study Acetone, Toluene, Cyclohexane, Butanol, Dichloromethane, 1,4-Dioxane, Hexadecane, Ethanol, Methanol, Pentadecane, Propanol, Hexane, Ethyl ether, and Trichloromethane solvents of HPCL grade procured from commercially available S-D fine chemicals Ltd. India are used without any further dilution.

Experimental Methods

The Uv-vis absorption studies were carried out on a Shimadzu UV-1800 spectrophotometer. Steady-state fluorescence studies were carried out on Hitachi F-2700 Fluorescence Spectrometer. The excitation wavelength is selected for recording the fluorescence emission spectra and obtained at the highest – intensity at more resolution. All measurements were performed at 273 K with solutions concentration are 10^{-5}–10^{-6} M. The solvent parameters dielectric constant (ε) and refractive index (n) of the `solvents are taken from the collected works [13–15].

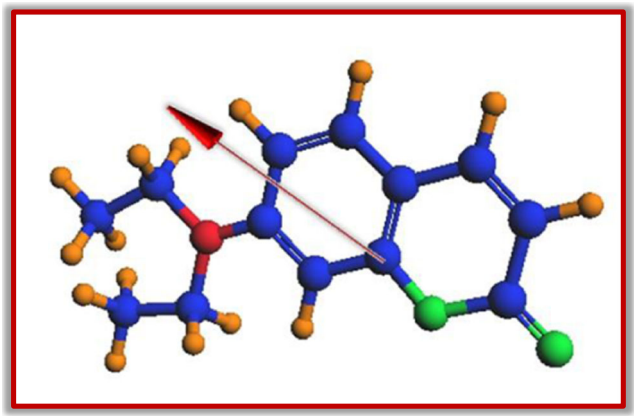

Fig. 1 Optimized molecular structure of Coumarin-466

Theoretical Context

To resolve the electric dipole moments of C-466, the absorption maxima (in cm^{-1}), fluorescence maxima (in cm^{-1}) and dipole moment ratios to the probe have been defined by following equations.

Method I

On the basis of various assumptions, the four independent equations, which are derived [16–19], to determine the dipole moment in excited state (μ_e) of the probe by means of,

Lippert-Mataga equation (LME) [16]

$$\tilde{\nu}_a - \tilde{\nu}_f = m_1 F_1(\varepsilon, n) + \text{constant} \quad (1)$$

Bakshiev's equation (BE) [17]

$$\tilde{\nu}_a - \tilde{\nu}_f = m_2 F_2(\varepsilon, n) + \text{constant} \quad (2)$$

Chamma-Viallet-Kawski's equation (CVKE) [18].

$$\frac{\tilde{\nu}_a + \tilde{\nu}_f}{2} = -m_3 F_3(\varepsilon, n) + \text{constant} \quad (3)$$

McRae's equation (MRE) [19]

$$\tilde{\nu}_a = -m_4 F_4(\varepsilon) + \text{Constant} \quad (4)$$

where $F_{1(LME)}(\varepsilon, n) = \frac{\varepsilon-1}{2\varepsilon+1} - \frac{\varepsilon-1}{2\varepsilon+1}$, $F_{2(BE)}(\varepsilon, n) = \frac{2n^2+1}{n^2+2}\left[\frac{2n^2+1}{n^2+2} - \frac{2n^2+1}{n^2+2}\right]$, $F_{3(CVKE)}(\varepsilon, n) = \left[\frac{2n^2+1}{2(n^2+2)}\left(\frac{2n^2+1}{2(n^2+2)} - \frac{2n^2+1}{2(n^2+2)}\right) + \frac{2n^2+1}{2(n^2+2)}\right]$ and $F_{4(MRE)} = \left[\frac{2(\varepsilon-1)}{\varepsilon+2}\right]$ are known as solvent polarity functions respectively. Table 1 contains all used solvent parameters and polarity functions. Using quantum mechanical perturbation theory above equations having absorption ($\tilde{\nu}_a$) maxima, fluorescence ($\tilde{\nu}_f$) maxima and Stokes shift (in wave numbers) in various solvent medium of different refractive index (n) and dielectric constant (ε) and where m_1, m_2, m_3 and m_4 are

$$m_1 = \frac{2\left(\mu_e - \mu_g\right)^2}{hca^3} \quad (5)$$

$$m_2 = \frac{2\left(\mu_e - \mu_g\right)^2}{hca^3} \quad (6)$$

$$m_3 = \frac{2\left(\mu_e^2 - \mu_g^2\right)}{hca^3} \quad (7)$$

$$m_4 = \frac{\mu_g\left(\mu_e - \mu_g\right)}{hca^3} \quad (8)$$

The notations c, h, μ_g and μ_e are velocity of light (in vacuum), Planck's constant, ground and excited states dipole moments respectively. The slopes m_1, m_2, m_3 and m_4 are obtained by plotting linear curve fitting for ($\tilde{\nu}_a$ - $\tilde{\nu}_f$) versus $F_1(\varepsilon, n)$, ($\tilde{\nu}_a$ - $\tilde{\nu}_f$) versus $F_2(\varepsilon, n)$, ($\frac{\tilde{\nu}_a+\tilde{\nu}_f}{2}$) versus $F_3(\varepsilon, n)$ and $F_4(\varepsilon)$ versus $\tilde{\nu}_a$ correspondingly. According to the Edward atomic increment method the Onsager radius (a) of solute molecule was estimated [20]. Both ground state and excited state dipole moments are calculated by the following equations.

$$\mu_g = \frac{m_3 - m_2}{2}\left[\frac{hca^3}{2m_1}\right]^{\frac{1}{2}} \quad (9)$$

$$\mu_e = \frac{m_3 + m_2}{2}\left[\frac{hca^3}{2m_1}\right]^{\frac{1}{2}} \quad (10)$$

$$\mu_e = \left[\frac{m_3 + m_2}{m_3 - m_2}\right]\mu_g \quad ; \quad m_3 > m_2 \quad (11)$$

If the μ_g and μ_e are not parallel to each state, which forms small angle φ and angle φ can be estimated as follows

$$\cos\varphi = \frac{1}{2\mu_g\mu_e}\left[\left(\mu_g^2 + \mu_e^2\right) - \frac{m_3}{m_2}\left(\mu_e^2 - \mu_g^2\right)\right] \quad (12)$$

The graphical plots of ($\tilde{\nu}_a - \tilde{\nu}_f$) and ($\frac{\tilde{\nu}_a+\tilde{\nu}_f}{2}$) against solvent polarity functions gives linear relations and their slopes. These formulas were based on certain assumptions by considering dipole moments of ground and excited state are co-linear for same molecular radius.

Table 1 Solvent parameters and solvent polarity functions

Solvent	ε	n	$F_1(\varepsilon,n)$	$F_2(\varepsilon,n)$	$F_3(\varepsilon,n)$	$F_4(\varepsilon)$	$E_T(30)$	E_N^T	α	β	π*
Hexane	1.890	1.375	0.00140	−0.00014	0.25510	0.458	31.0	0.0092	0	0	0.11
Cyclohexane	2.020	1.426	−0.00158	−0.00127	0.28740	0.507	30.9	0.0061	0	0	0
Pentadecane	2.039	1.431	−0.00102	0.00201	0.29134	0.514	–	–	–	–	–
Hexadecane	2.046	1.434	−0.00119	−0.00240	0.29310	0.517	–	–	0	0	0.08
Toluene	2.379	1.497	0.01311	0.02879	0.34980	0.630	33.9	0.0987	0	0.1	0.49
1,4 Dioxane	2.210	1.421	0.02094	0.04238	0.30693	0.575	36.0	0.164	0	0.37	0.49
Ethyl ether	4.335	1.352	0.16708	0.37724	0.42829	1.053	34.5	0.1172	0	0.47	0.24
Trichloromethane	7.430	1.430	0.19300	0.54780	0.60090	1.364	35.9	0.16	0	0	0.49
Dichloromethane	8.930	1.424	0.21800	0.63000	0.58520	1.451	40.7	0.32	0.13	0.1	0.73
Butanol	17.10	1.397	0.26330	0.74710	0.64337	1.686	49.7	0.6018	0.84	0.84	0.47
Propanol	20.80	1.385	0.27492	0.78260	0.65316	1.737	50.7	0.6172	0.84	0.9	0.52
Acetone	20.70	1.359	0.24650	0.79028	0.63952	1.736	42.2	0.3549	0.08	0.48	0.67
Ethanol	25.30	1.361	0.28976	0.81676	0.65410	1.780	51.9	0.6543	0.86	0.75	0.54
Methanol	33.00	1.328	0.30894	0.85533	0.65133	1.829	55.4	0.7623	0.98	0.66	0.60

Method II

The empirical polarity parameter E_N^T versus spectral shifts by Reichardt [21], the dipole moment of excited state molecule can be calculate as follows,

$$\tilde{\nu}_a - \tilde{\nu}_f = 11307.6\left[\left(\frac{\delta\mu}{\delta\mu_B}\right)^2\left(\frac{a_B}{a}\right)^3\right]E_N^T + const \quad (13)$$

where '$\delta\mu_B$' the difference in dipole moment and 'a' Onsager cavity radius of chosen molecule. The '$\delta\mu$' can be measured as

$$\delta\mu = \mu_e - \mu_g = \sqrt{\frac{m\,x\,81}{11307.6(6.2/a)^3}} \quad (14)$$

Where, 'm' is the slope of linear graph of Stoke shift versus E_N^T microscopic solvent polarity.

We have also examined the Solvatochromic investigation of C-466 within the sight of different solvents using Solvatochromic model which deals the solute-solvent interaction. We used Kamlet-Taft (KT) model [22, 23].

$$A = A_0 + s\pi^* + a\alpha + b\beta \quad (15)$$

where 'A' is the spectral peak frequency of molecule in solvents, 'A_0' for frequency peak position of the solute in vapour state, π^* signifies polarity, α for Hydrogen Bond Donor (HBD) and β for Hydrogen Bond Acceptor (HBA) properties of the solvents where 's', 'a' and 'b' are the coefficients obtained from linear regression method. Solvents parameters π^*, α and β are taken from literature report [13–15].

Result and Discussion

Solvent Effects on Absorption and Fluorescence Spectra

The absorption spectra and fluorescence emission spectra of C-466 in dissimilar solvents are shown in Figs. 2 and 3. The wavenumbers of absorption and fluorescence emission maxima of the coumarin molecule in varies solvents are reported in Table 2. Table 2 also contains the selected solvents Stokes shift data, by which the proportion of excited state to the ground state dipole moments can be ascertained. From Fig. 2, C-466 spectrum in various solvents are tranguil of different bands in the range 340–390 nm. It apparent that, the structure of the C-466 and polarity of the intermediate each are of immense significance to an influence on spectral behaviour of the laser dye [24]. The highest wavelength of absorption maximum 385 nm for propanol and lowest absorption maximum 351 nm for hexane. The shape of the spectrum for all solvents follows same trend but only in cyclohexane, hexadecane and pentadecane solvents shows dual peaks. The fluorescence spectra of C-466 in all studied solvents as in Fig. 3 reveal wavelength range 390–460 nm. From fluorescence data, C-466 in 1,4-dioxane, toluene, cyclohexane, butanol and propanol solvents shows highest intensity. As in methanol, C-466 has least intensity of fluorescence. From both the absorption and emission spectrum of C-466, noted that the bathochromic(red-shift) observed in all the solvents. These bathochromic shifts are obtained by increasing polarity of solvents suggest that the transitions convoluted $\pi \rightarrow \pi^*$. Such kind of spectral shifts are in general, due to the interactions of solvent and solute molecules, which might be possibly of general type or specific type such as Hydrogen bonding.

The general type of solvent effect depends on the refractive index and dielectric constant of solvents parameters, whereas the specific effects are related by means of π-donor, n-donor and Hydrogen bonding ability of the solvents. Intended for

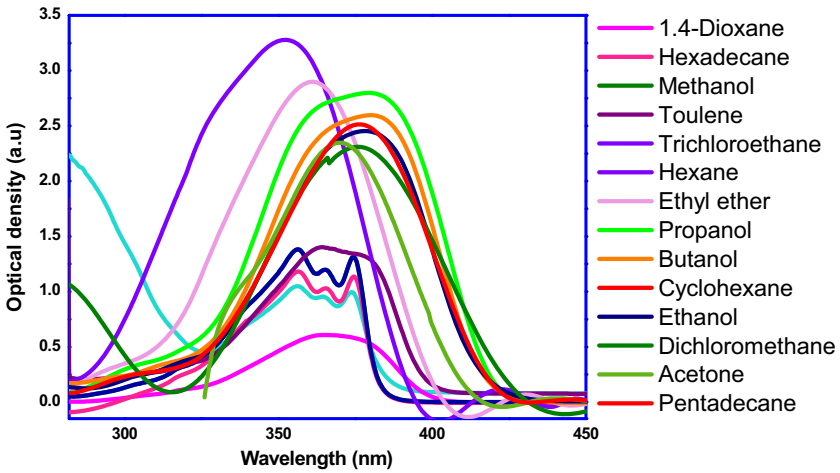

Fig. 2 UV-vis spectrum for Coumarin-466 for all studied solvents

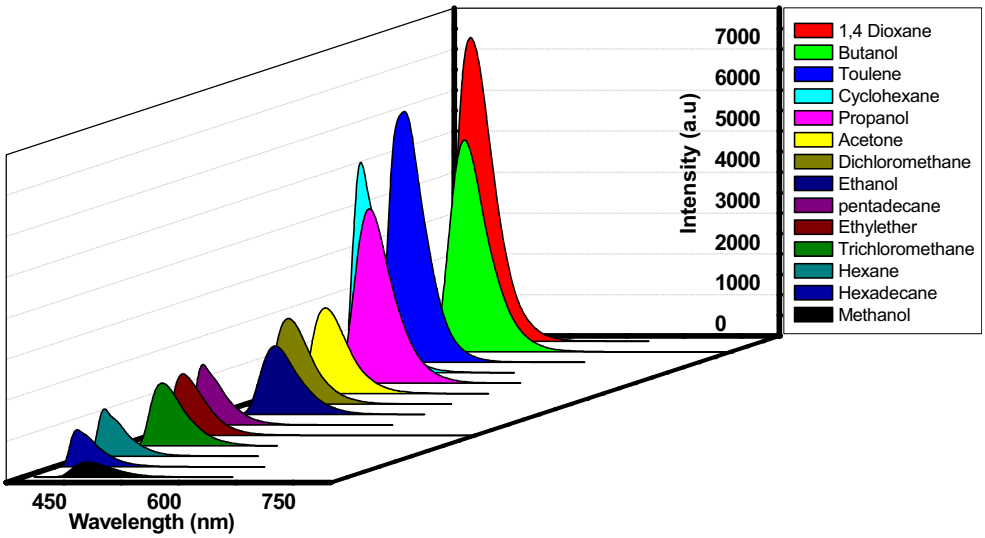

Fig. 3 Fluorescence spectra for Coumarin-466 in all studied solvents

polar solutes molecules the interface with non-polar solvents be subject to the dipole-induced-dipole forces, although with aprotic solvents, the solvent-solute interaction be influenced by the resilient dipole-dipole forces. In protic solvents in adding to dipole-dipole interplays, specific interaction, such as Hydrogen bonding might be operative as the Intermolecular Charge Transfer (ICT) character favourable Hydrogen bonding along with hydroxyl group in alcohol solvents. Hydrogen bonding interaction generally sets a simple constraint on the validity of the Eqs. (1–3). The dependence of Stokes shift, $\tilde{\nu}_a - \tilde{\nu}_f$ on solvent polarity as given by Lippert's manifestation appears to be less consistent within solvents. This tendency can possible because of the fact that, the Lippert's equation disregards the molecular characteristic of solvation. It is thusly convenient as pointed out by others besides [24, 25] to use ΔF ([ΔF = (ε-1)/(2ε+1)-(n^2–1)/ (2n^2 + 1)]) parameter which is an experiential quantity of solvent polarity for considerate the polarization dependency of spectral individualities. Figures 4, 5 and 6 are shows the absorption maxima, fluorescence emission maxima and Stokes shift versus ΔF. As understood from these Figs. 4, 5 and 6 the absorption and fluorescence emission maxima are linearly correlated to ΔF for only selected solvents. Here we used only selected solvents, because the reason that other solvents are deviated from the linearity due to specific interaction effects by hydrogen bonding ability of solvents. The residual square R^2 of the graph for

Table 2 Electronic absorption and fluorescence spectra of studied compound

Solvent	λ_a	λ_f	$(\tilde{\nu}_a)$	$(\tilde{\nu}_f)$	$(\tilde{\nu}_a - \tilde{\nu}_f)$	$(\tilde{\nu}_a + \tilde{\nu}_f)$	$(\tilde{\nu}_a + \tilde{\nu}_f)/2$
Hexane	351	398	26,881.78	25,725.62	1756.10	52,007.34	26,003.67
Cyclohexane	373	399	26,809.65	25,062.65	1747.00	51,872.30	25,936.15
Pentadecae	374	402	26,737.96	24,875.62	1862.34	51,613.58	25,806.79
Hexadecane	374	405	26,737.96	24,691.35	2046.61	51,429.30	25,714.65
Toluene	374	414	26,704.94	24,154.58	2570.45	50,879.52	25,439.76
1,4 Dioxane	373	417	26,774.02	23,980.81	2793.21	50,754.83	25,377.45
Ethyl ether	362	417	26,809.65	23,980.81	2828.84	50,790.46	25,395.23
Trichloromethane	378	432	26,455.02	23,148.14	3306.88	49,603.16	24,801.58
Dichloromethane	374	430	26,737.96	23,255.81	3482.15	49,993.77	24,996.88
Butanol	378	451	26,455.02	22,172.94	4282.08	48,627.96	24,313.98
Propanol	385	452	25,974.02	22,123.89	3850.13	48,097.90	24,048.95
Acetone	372	436	26,881.72	22,935.77	3945.95	49,817.48	24,908.74
Ethanol	378	455	26,455.02	21,978.02	4477.00	48,433.04	24,216.52
Methanol	381	460	26,246.71	21,739.13	4507.58	47,985.80	23,992.90

λ_a and λ_f wavelength of Absorption and fluorescence maxima (nm)

$\tilde{\nu}_a$ and $\tilde{\nu}_f$ wavenumber of absorption and fluorescence emission maxima (cm^{-1})

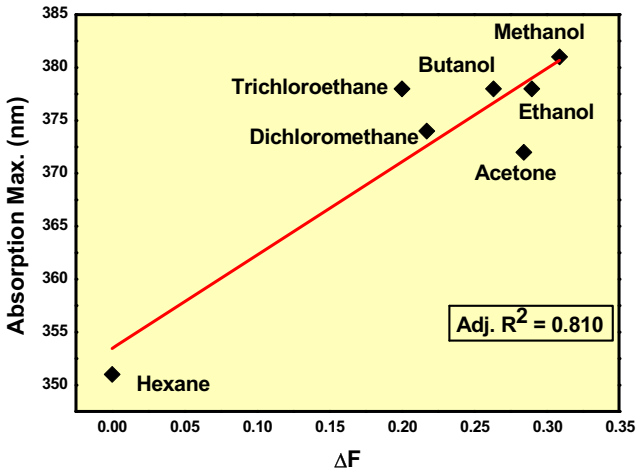

Fig. 4 Absorption max. Versus solvent polarity parameter for Coumarin-466 in selected solvents

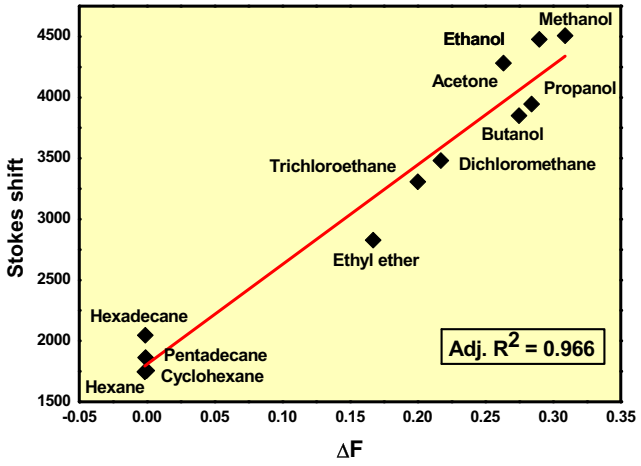

Fig. 6 Stoke shift versus solvent polarity parameter for Coumarin-466 in selected solvents

fluorescence emission is more linearity (0.931) as compared to absorption maxima (0.810) this implies that the studied coumarin dye, solvation is large in S_1 state compared to that in ground state [25]. In other words, the dipole moments in excited state is larger compared to ground state ($\mu_e^* > \mu_g$). The linear dependence of Stokes shift ($R^2 = 0.966$) on ΔF categorizes the existence of general kind of solvent-solute interaction.

Assessment of Ground and Excited State Dipole Moments

Towards quantify the statement that, $\mu_e^* > \mu_g$, we calculated the ground state dipole moment (μ_g) and excited state dipole moment (μ_e^*) for C-466 dye calculated using Lippert-Mataga [16] Bakhshiev [17] Chamma-Viallet-Kawski [18] and McRae [19] relations. Solvent shift data for coumarin dye is presented in Tables 1 and 2 and plots of $\tilde{\nu}_a - \tilde{\nu}_f$ versus $F_{1(LME)}$ (ε, n), $\tilde{\nu}_a - \tilde{\nu}_f$ versus to $F_{2(BE)}$ (ε, n), $\tilde{\nu}_a + \tilde{\nu}_f/2$ versus to $F_{3(CVK)}$ (ε, n), $\tilde{\nu}_a$ versus $F_{4(MRE)}$ and $\tilde{\nu}_a - \tilde{\nu}_f$ versus to solvent polarity function E_T^N are shown in Figs. 7, 8, 9, 10, 11 and 12 using least square fit method [26, 27] are used to calculate the above assessments. As can be seen from the figures, for some solvents deviation from the linearity is observed and this feature is ascribed to the approximation made in the specific solvent-solute interaction and/or solvatochromic shift method. To minimize these deviations, we chose some selected Stokes shift to get good a correlation between the shifts and solvent polarities. The data statistical treatments from all methods viz. the slopes, intercept, correlation co-efficient and number of data are presented in Table 3. Obtained correlation coefficients from the graphical data are larger than 0.845 residual square, which represents a linear relationship of correlations. Substituting the values of m_1, m_2, m_3, and m_4 of

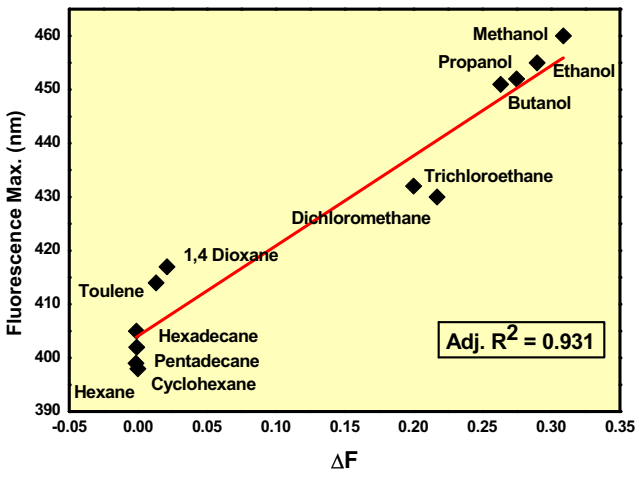

Fig. 5 Fluorescence max. Versus solvent polarity parameter for Coumarin-466 in selected solvents

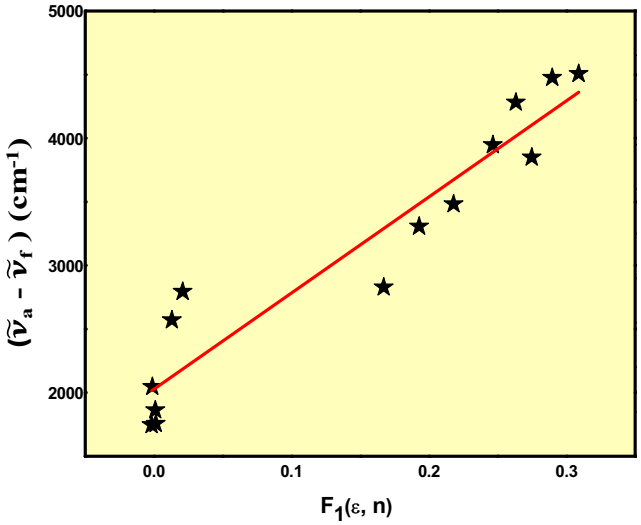

Fig. 7 A plot of ($\tilde{\nu}_a - \tilde{\nu}_f$) function versus F_1 (ε, n) of Coumarin-466

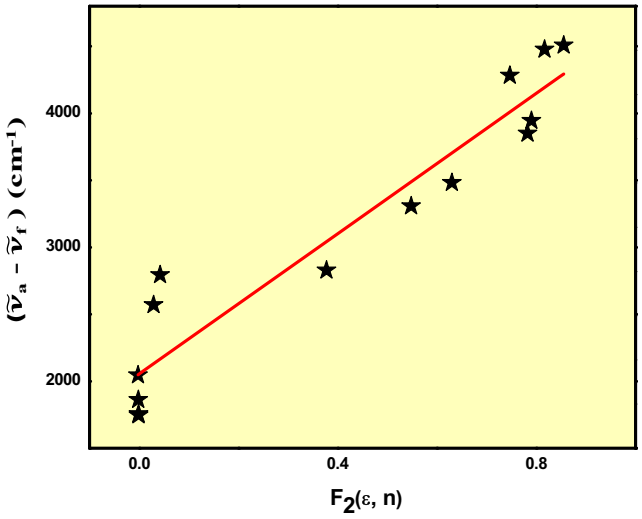

Fig. 8 A plot of $(\tilde{\nu}_a - \tilde{\nu}_f)$ function versus F_2 (ε, n) of Coumarin-466

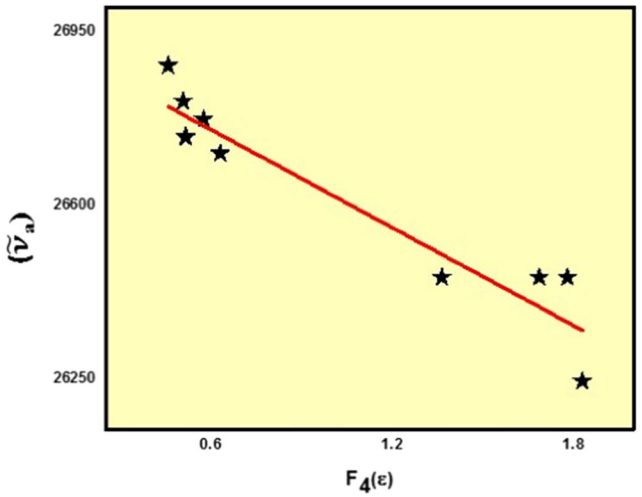

Fig. 10 A plot of $(\tilde{\nu}_a)$ function versus F_4 (ε) of Coumarin-466

the compound obtained from the slopes of Figs. 7, 8, 9, 10, 11 and 12 in Eqs. (5–8) and (15) to get the μ_e^* for C-466 [28, 29]. The correlation co-efficient are greater than 0.91, indicating a better linearity. Table 3 contains the values of slopes m_1 and m_2 of the fitted lines and the correlation factor (r). From Eqs. (5–8) and (14), the results obtained for ground state, excited state dipole moment, change in dipole moment and ratio of dipole moments are tabulated in Table 4.

The increase of values in the excited state dipole moment as obtained is revealing of the order of magnitude of the change and not the exact value due to the limitations set by the assumptions made while deriving the relations. All of these results are reported in Table 4. For C-466 it is found that $\mu_e^* > \mu_g$, i.e. the excited state dipole moment is higher compared to that in the ground state for all methods, a great Intermolecular Charge Transfer (ICT) in the excited state solidifies the molecule more polar in excited state as compared to the ground state. The variance among ground state and excited state dipole moments are ranged from 1.435–6.342D. This represents C-466 coumarin is more polar in excited state as compared to the ground state due to redistribution of charge and change in geometry of C-466 in excited state [30, 31].

For the compound coumarin (C-466), the slopes of Figs. 7 and 9 were originate to be $m_2 = 2617.50$ cm^{-1}, $m_3 = 3445.76$ cm^{-1} and radius of solute molecule was calculated (a = 3.6 Å). As a result of using Eqs. 9 and 10, we get $\mu_g = 0.5621$D, $\mu_e^* = 4.1157$D and $\Delta\mu = \mu_g - \mu_e^*$ is 7.332D. Starting the Eqs. 9 and 10 the dipole moments μ_g (ground state) and μ_e^* (excited state) be subject to not only on m_1 and m_2 but also on solute radius. Figures 7 and 9 shows the spectral shift of $(\tilde{\nu}_a - \tilde{\nu}_f)$ and $(\tilde{\nu}_a - \tilde{\nu}_f)/2$ of C-466 in various solvents vs. solvent polarity parameter. The obtained results of

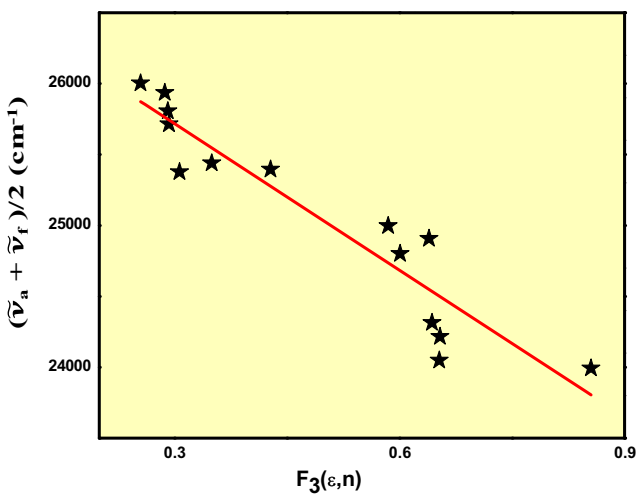

Fig. 9 A plot of $(\tilde{\nu}_a - \tilde{\nu}_f)/2$ function versus F_3 (ε, n) of Coumarin-466

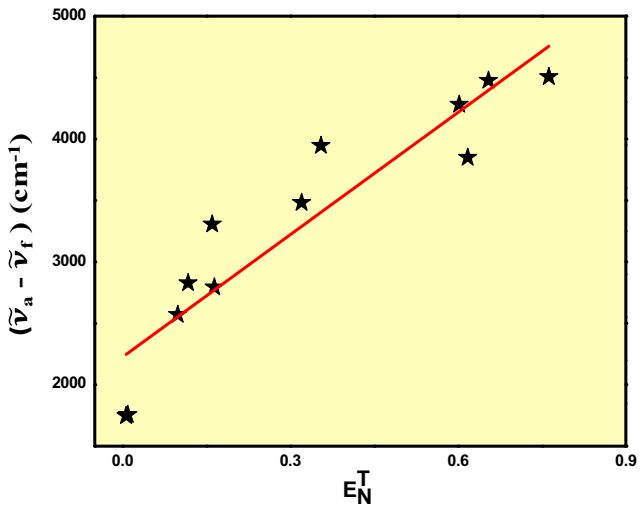

Fig. 11 A plot of $(\tilde{\nu}_a - \tilde{\nu}_f)$ function versus E_N^T of Coumarin-466

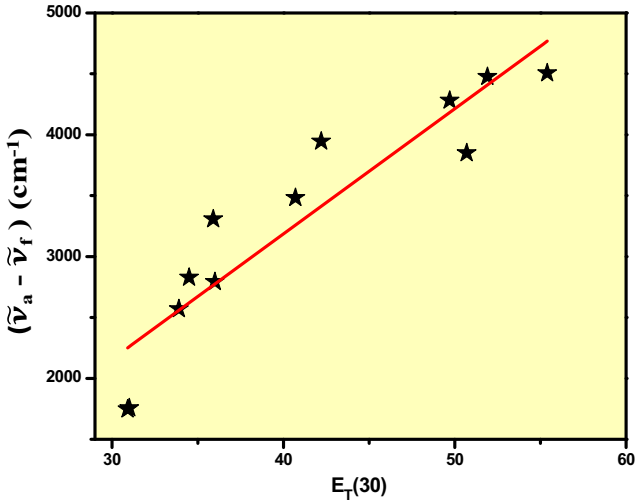

Fig. 12 A plot of ($\tilde{\nu}_a$ - $\tilde{\nu}_f$) function versus $E_T(30)$ of Coumarin-466

μ_g (ground) and μ_e* (excited) for this Coumarin dye are positive, which signifies that the excited state is more polar [32, 33]. Besides, it is determines the excited state electronic charge appropriation ought to be considerably not quite the same as the ground state charge appropriation. By estimating the surface area of the molecule as sphere-shaped, based on absorption maxima and fluorescence maxima band shifts in various solvents, μ_e*/μ_g can be determined. Similarly, the current study using Eq. 11 to estimate the value of the excited state by pre facts of the value of ground state, short of the necessity to knowing the molecular radius.

The Hydrogen bonding ability and solvent polarity dependence of C-466, are calculated using Kamlet-Taft relation. To obtain the knowledge about each contributions of HBD and HBA ability of solvents on the spectroscopic parameters of $\tilde{\nu}_a$,$\tilde{\nu}_f$ and $\Delta\tilde{\nu}$ (= $\tilde{\nu}_a$ -$\tilde{\nu}_f$). These are related to the solvatochromic factors α, β & π* properties of solvents. To get these values we use the multilinear regression analysis (MLRA) [34]. The measurement of MLRA results along with co-efficient are presented in the below relation form.

$$\tilde{\nu}_a\ (\mathrm{cm}^{-1}) = 26829.75 - 151.38\pi^* - 503.670\alpha + 116.010\beta\ (\mathrm{Adj.R}^2 = 0.894)$$
$$\tilde{\nu}_f\ (\mathrm{cm}^{-1}) = 24267.68 + 321.01\pi^* - 1452.65\alpha - 1025.12\beta\ (\mathrm{Adj.R}^2 = 0.975)$$
$$\Delta\tilde{\nu}\ (\mathrm{cm}^{-1}) = 25319.18 + 1762.65\pi^* + 2024.68\alpha - 478.700\beta\ (\mathrm{Adj.R}^2 = 0.965)$$

The absorption and emission spectra (ν_{max}) values in gas phase show a discrepancy and the polarizability parameters (s) intensifications from the μ_g to μ_e* which indicates the molecular stability. It is observed from the above relatives that, the nonspecific dielectric interaction (π*) has the strong solvent influence on the molecule. Above relation shows that HBD (α) stimuluses more than HBA (β) for $\tilde{\nu}_a$ and $\tilde{\nu}_f$, where as in $\Delta\tilde{\nu}$, HBD (α) effect is higher than HBA (β).

Computational Details

To obtain the extra enlightenment of the molecular electronic properties for C-466, we examined hypothetical Ab initio quantum mechanical calculations which were executed in GAMESS [35] performed time-dependent DFT (TD-DFT) using BECKE-1998 (exchange)/STO-6G basis set. The ground Highest Occupied (HOMO) and Lowest Unoccupied (LUMO) Molecular Orbital were calculated in vacuum and in solvent medium. The Molecular Electrostatic Potential (MEP) and Solvent Accessible Surface (SAS) were also analysed. The absorption energy's, orbital contributions and oscillator energy towards the minimum ten levels of singlet-singlet transits in optimized geometry of the ground condition were acquired through ZINDO-CI computations employing the identical basis set in regard to optimised geometry.

Table 3 Statistical data of linear plots for different correlation methods of studied compound

Method	Slope (cm^{-1})	Intercept	Correlation coefficient (r)	No. of data
Lippert-Mataga correlation	7553.53	2027.58	0.92881	14
Bakhshieve's correlation	2617.50	2054.97	0.91136	14
Kawski-Chamma-Viallet	3445.76	26,752.2	0.87414	14
McRae	328.280	26,949.4	0.89170	09
E_N^T correlation	3318.43	2226.48	0.84840	12
$E_T(30)$	102.800	926.860	0.84500	12

Table 4 Onsager cavity radius, ground state and excited state dipole moments of C-466 (in Debye)

Compound	C-466
Onsager radius Å	3.6484
μ_g [a] (D)	0.5621
μ_e [b] (D)	4.1157
μ_e [c] (D)	1.9970
μ_e [d] (D)	6.9041
μ_e [e] (D)	4.0293
μ_e [f] (D)	1.9990
$\Delta\mu$ [g] (D)	6.3420
μ_e /μ_g [h] (D)	7.3220
φ [i] (rad)	1.5689

[a] Ground state dipole moment

[b] Excited state dipole moment calculated from Kawski-Chamma-Viallet Equation

[c] Excited state dipole moment calculated from Bakhshieve's Equation

[d] Excited state dipole moment calculated from Lippert-Mataga Equation

[e] Excited state dipole moment calculated from E_N^T Equation

[f] Excited state dipole moment calculated from McRae Equation

[g] Change dipole moment from μ_e and μ_g

[h] μ_e /μ_gThe ratio of excited state and ground dipole moment

[i] φ The orientation of the molecule in excited state w.r.t ground state

Molecular Orbital Study

To acquire more information about molecular arrangement and its phyisco-chemical properties of C-466, We have performed theoretical computations using GAMESS [35]. Quantum mechanical Time dependent Density Functional Theory (TDDFT)with STO-6G basis set has been used to achieve (a) Optimised Structure (b) HOMO-LUMO orbitals (C) MEP and (D) SAS in both ethanol and vacuum media. The 3D pictures of Frontier orbitals HOMO-LUMO for C-466 in vacuum and ethanol are depicted in Fig. 13, From the Table 5 we infer that, there is a minor change in the values of oscillator strength for probe molecule studied both in vacuum and ethanol. The dipole moment values in ethanol media compared to vacuum there is a significant change which implies that charge distribution in ethanol is more compared to vacuum.

For HOMO in vacuum the electrons are strongly localized C2, C3, C4, C5, C7, C8, C9, C10, O11 of carbon and oxygen atoms, and least localized on N12 nitrogen atom. In ethanol media the electrons are partly located at C2, C4, C9, C8, H23 carbon and hydrogen atoms. The LUMO orbitals both in vacuum and ethanol are located at the same C1, C2, C3, C10, C8, C5, C6 and O11 atoms [36–38]. There are no significant changes observed in LUMO+2 and LUMO+1 in vacuum except localized on O11 oxygen atom. In ethanol media localization of electrons occurs in two different benzene rings for LUMO+2 and LUMO+1 orbitals. In C-466 HOMO-1 in vacuum and HOMO-1 in ethanol localization are on same carbon atoms (C5, C7, C9, C10). Only HOMO-2 orbital in ethanol localization of electrons seen in C15, H27, H28, C16, H30, H31 atoms of dimethylamine group. Based on the optimized geometry, molecular orbital analysis for studied molecule, we observe from the Table 5 energy gap is very small (0.2702 eV in vacuum and 0.2098 eV in ethanol) which indicates π-π^* transitions is easier, further probe molecule is more susceptibility and high chemical reactivity [39, 40]. By using HOMO and LUMO energies we determined chemical quantities of sample properties and atomic/molecular properties [40]. In basic molecular orbital theory, the HOMO energy was associated to the Ionization potential (Z) and the LUMO energy analyse the electron affinity (E) correspondingly by the succeeding form: $Z = E_{HOMO}$ and $E = E_{LUMO}$. The hardness of the molecule (η) = (Z-E)/2. The softness of the molecule is inverse of the hardness (S) = 1/2η. The chemical potential (μ) = − (Z + E)/2. The electrophilicity index (ω) = μ^2/2 η. The electronegativity (χ) = (Z + E)/2. These chemical quantities calculated both in vacuum and ethanol media and results are tabulated in Table 6. Molecular orbital states energies for C-466 in different medium as listed in Table 6, It is observed small energy values of HOMO-LUMO, a molecule with small orbital energy gap is known as excitation energy which implies π-π^* transitions is easier, high chemical reactivity of molecule towards electron transfer and newly employed to establish the bioactivity from ICT (intramolecular charge transfer) [46–48] together low kinetic stability.

Solvent Accessible Surfaces

Solvent accessible surface (SAS) indicates active regions of the probe with the solvent molecules. SAS for the sample C-466, both in vacuum and in ethanol media with the contour values ranging from −0.331 to 0.203 are depicted in the Fig. 14 adopting BECKE-1998(exchange)/STO-6G basis set in GAMESS program. The green surface is spread over the entire molecule of C-466 suggests that entire molecule is active in solvent. The robust interactions site of sample is found to be at ester group with the surrounding media [41, 42].

Molecular Electrostatic Potential

Electronic charge density describes the electron cloud magnitude of the molecules. Calculated electron densities of C-466 molecule by using DFT/BECKE-1988 (exchange)/STO-6G in vacuum and in ethanol are represented in Fig. 15. According to electron density on

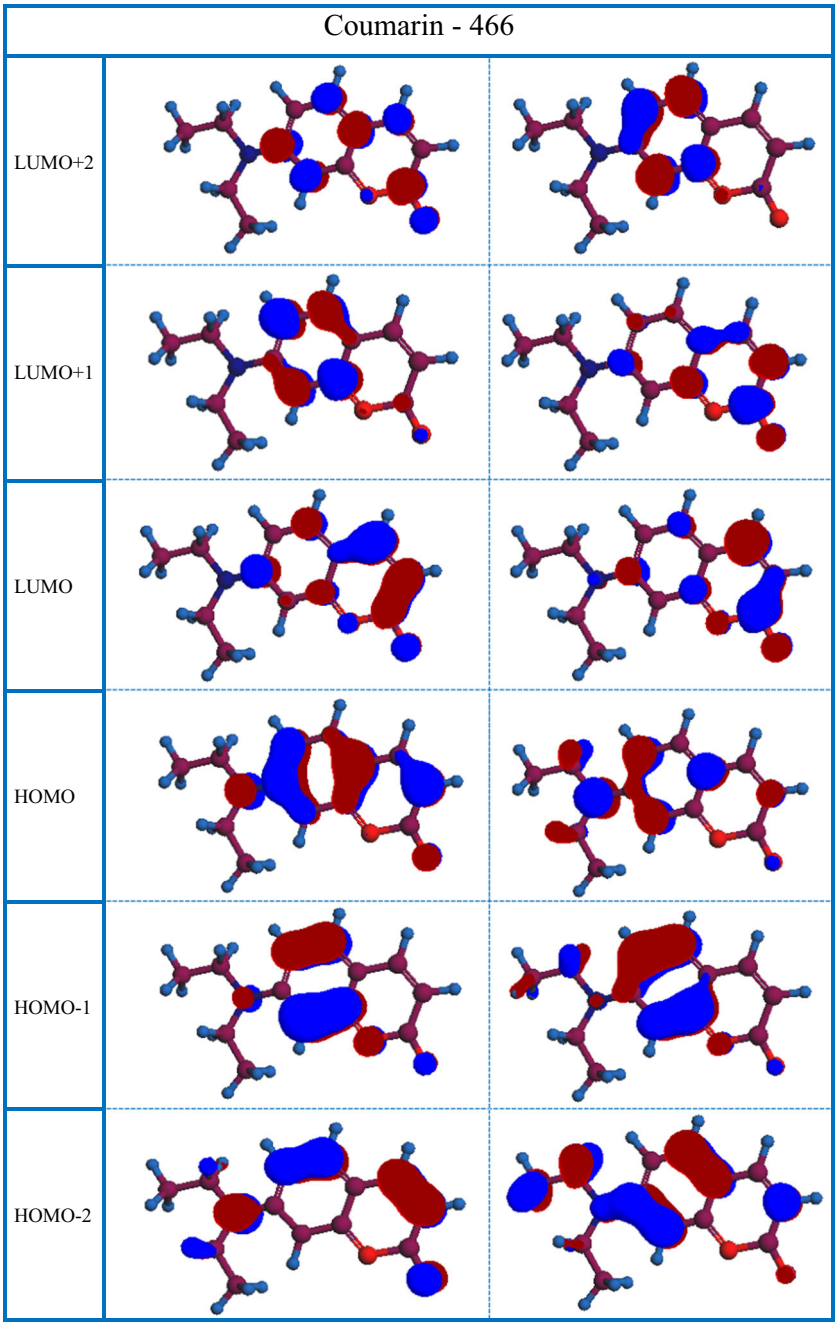

Fig. 13 Plots of Molecular Orbitals for Coumarin-466

Table 5 HOMO and LUMO energy details for C-466 in Vacuum and Ethanol media

Orbital	Energy in eV		Orbital states	Oscillator strength		Dipole in Debye	
	Vacuum	Ethanol		Vacuum	Ethanol	Vacuum	Ethanol
L + 2	0.02624	0.045889	H → L	0.8204	0.6002	14.010	32.9150
L + 1	0.01426	0.010722	H-2 → L	0.3518	0.2184	15.438	31.5796
L	−0.02623	−0.04640	H-1 → L	0.0847	0.0463	14.547	28.9459
H	−0.29647	−0.2562	H → L + 1	0.3737	0.3435	6.3948	33.3055
H-1	−0.33306	−0.30956	H → L + 2	0.1740	0.1252	11.187	21.8795
H-2	−0.36644	−0.32551	H-2 → L + 1	0.0464	0.1582	7.5919	32.0506

Table 6 Physico-Chemical properties for C-466

Parameters (eV)	C-466	
	Vacuum	Ethanol
HOMO Energy	−0.29647	−0.2562
LUMO energy	−0.02623	−0.0464
Energy Gap	0.27024	0.2098
Electro negativity	−0.16135	−0.1513
Chemical potential	0.16135	0.1513
Global hardness	−0.13512	−0.1049
Electrophilicity	−0.09633	−0.1091
Global softness	−3.70041	−4.7664

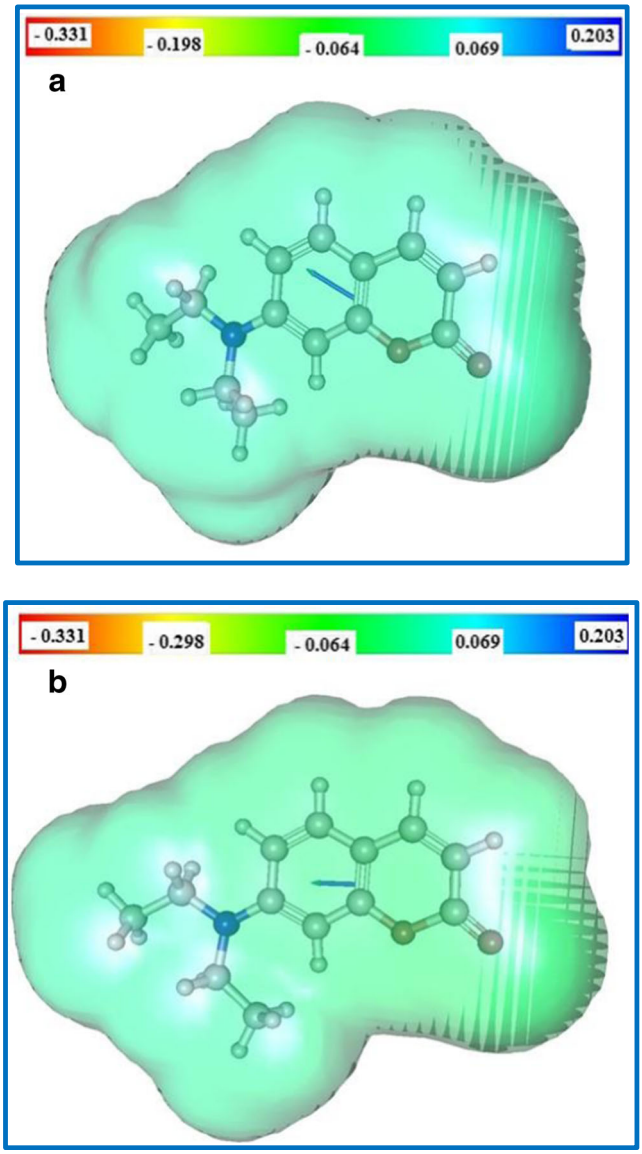

Fig. 14 3D plots of solvent accessible surfaces for Counarin-466 (A) in Vacuum and (B) in Ethanol solvent

various points of the molecule, helps in knowing the location of nucleophilic reactions, electrophilic strikes in addition to hydrogen bonding interactions within solvents. Different value of electrostatic potential in the exterior are exhibited with dissimilar colours. The negative (Red) area has been associated to electrophilic reactivity, positive (Blue) area to nucleophilic reactivity, and neutral (Green) area [43–45]. For C-466 contour values are in the range − 0.0298 to 0.0298 in vacuum and − 0.0625 to 0.0625 in ethanol. In vacuum and ethanol electrophilic reactivity are predominantly localized on O-11 oxygen atom. Nucleophilic reactivity is spread almost entire molecule for both in vacuum and ethanol. Neutral region is spread more in ethanol than vacuum on second ring structure. The magnitude of electron density is found to be more on oxygen atom, followed by nitrogen, carbon and hydrogen atoms. In ethanol solvent, solvent interactions on C-466 results is decrease in electron densities on most of the atoms. Molecular orbitals are used to study the data about the charge transfer within the sample for both in vacuum and ethanol solvent media [46, 47].

Mulliken Atomic Charge Distribution Studies

The atomic charge distribution of an organic molecule characterises the charges of each and every atom within the molecule. The literature studies exhibit atomic computations gave a vital function in the utilisation of chemical estimation to molecular system due to atomic charges, electronic structure, acidity-basicity, molecular polarizability, dipole moment role and numerous characteristics of molecular system. Atomic charges of each and every atom of C-466 has been examined in vacuum and ethanol solvent to yield knowledge about electrical dipole moment originating from non-uniform charge dissemination [48, 49]. Electron density and Mullikan atomic charge distribution in vacuum and ethanol for C-466 are tabulated in Table 7. The improved pattern of Electron density and Mullikan atomic charges has been visualized graphically in Fig. 16, for C-466 in vacuum with atom number (C2, C3, C4, C7, C9, C10, C12, C14) carbon atoms (N12) nitrogen atom, (O6, O11) oxygen atoms exhibit negative charge (electron donor) though (C1, C5, C8, C13, C15) carbon atoms and all hydrogen atoms exhibits positive charge (electron acceptor). In ethanol medium, an increase in atomic charge of most of hydrogen atoms, slight increase in atomic charge of (C2, C3, C7, C15) carbon atoms. There is a drastic increase of atomic charge of (N12) nitrogen atom in ethanol than in vacuum [42, 50–53]. O6 and O11 oxygen atoms have opposite trend in vacuum and ethanol. The charge distribution either in vacuum and ethanol solvent indicates their occurrence in substantial polar character, directive from C1 (Q = 0.5715) to O11 (Q = −0.6091) atom for C-466. Such a charge

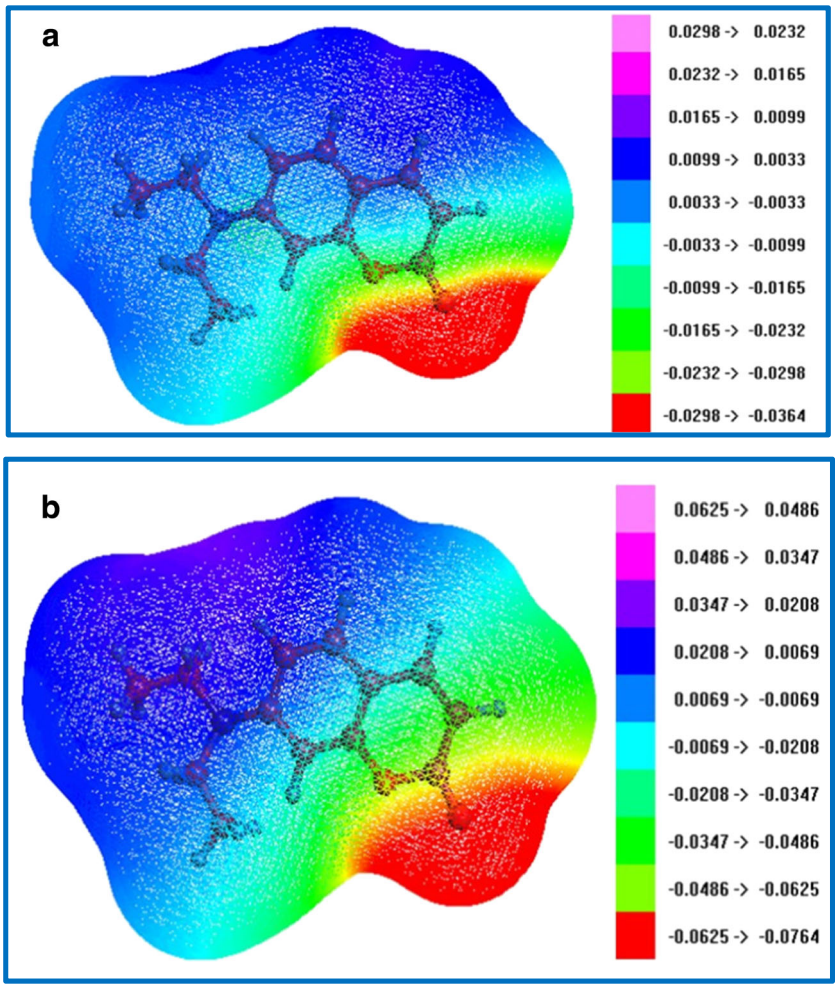

Fig. 15 Molecular Electrostatic Potential for Coumarin-466 (A) in Vacuum and (B) in Ethanol

shift is attributed to the discrepancy between ground and first excited dipole moment states. Only positive values of hydrogen atoms imply the charge shifts from H-atom to other atoms.

Photoluminescence Properties of C-466

The effective advancement of OLEDs depends on the ability to acquire outflow over the full visible range. OLEDs transmit different colours relying upon the transmitting fluorescent colours utilized, which are likewise the key materials influencing the luminance, proficiency, turn-on voltage and lifetime. In visible region light is made primarily out of three added substances essential colours, blue 435.8, green 546.1 and, red 700 nm, respectively from which it is conceivable to get different colours. As to shading, the human visualization reacts to trichromatic lifts on the virtual cortex, assessed by the Commission Internationale de L'Eclairage (CIE) in three coordinating limits or powerful spectral bands, A(λ), B(λ) additionally C(λ), open as free-get to tables. Chromaticity outline is a graphical portrayal of tristimulus values, which describe conceivable colours, shaped by a triangle with vertices controlled by colours value [54]. The 'A' and 'B' CI facilitates for the fluorescence emission of C-466 in different polarity solvents, were figured by Eqs. (16) and (17) from their x, y and z tristimulus integrations of Eqs. (18–20). Using photoluminescence results it is conceivable to make a graph of integrated PL intensity for each solvents, as appeared in Fig. 17.

$$A = x/(x + y + z) \tag{16}$$

$$B = y/(x + y + z) \tag{17}$$

$$x = \int_{250}^{750} I\,(\lambda)\,\overline{A}\,(\lambda)d\lambda \tag{18}$$

$$y = \int_{250}^{750} I\,(\lambda)\,\overline{B}\,(\lambda)d\lambda \tag{19}$$

$$z = \int_{250}^{750} I\,(\lambda)\,\overline{C}\,(\lambda)d\lambda \tag{20}$$

Table 7 Mulliken atomic charges (a.u) and electron density (a.u) of C-466 molecule in vacuum and ethanol

Atoms	DFT (in vacuum)		TDDFT (in ethanol)	
	Electron density	Atomic charge	Electron density	Atomic charge
1C	5.91621	0.5715	5.92656	0.1335
2C	6.03497	−0.0608	6.03325	−0.1152
3C	6.11494	−0.0285	6.10665	−0.1494
4O	8.13279	−0.0040	8.12504	0.0030
5C	6.06455	0.1815	6.06639	0.1415
6C	6.05857	−0.3398	6.05785	−0.3607
7C	5.91778	−0.0915	5.92272	−0.0982
8C	5.82093	0.1543	5.83812	0.2171
9C	6.09378	−0.0924	6.08974	−0.0323
10C	6.10369	−0.0657	6.09913	−0.0483
11 N	7.19991	−0.6091	7.19744	−0.4190
12O	8.18981	−0.3754	8.1977	−0.2368
13C	6.02801	0.0242	6.02639	0.0195
14C	6.02964	−0.1469	6.02617	−0.1365
15C	6.18502	0.0154	6.18538	0.0284
16C	6.18619	−0.1487	6.18512	−0.1461
17H	0.92459	0.0981	0.93186	0.0493
18H	0.9378	0.0892	0.93175	0.1055
19H	0.9328	0.1070	0.92404	0.0936
20H	0.94196	0.0743	0.93307	0.1331
21H	0.92802	0.0755	0.92511	0.1022
22H	0.92545	0.0637	0.92181	0.0957
23H	0.92568	0.0600	0.92128	0.0900
24H	0.92436	0.0585	0.92181	0.0413
25H	0.92467	0.0626	0.92115	0.0406
26H	0.92252	0.0458	0.93289	0.0480
27H	0.92688	0.0627	0.92899	0.0901
28H	0.92252	0.0604	0.93037	0.0858
29H	0.92955	0.0541	0.93075	0.0625
30H	0.92632	0.0578	0.92898	0.0635
31H	0.93007	0.0459	0.932497	0.0983

A Coumarin-466 is self-colourless solution. At 385 nm excitation a CIE chromaticity coordinates value x = 0.14–0.16 and y = 0.10–0.16, for C-466 in alcohols solvents (Butanol, Ethanol, Methanol and Propanol) generates near bluish green colour. For other solvents in studied compound which is deep blue colour with CIE coordinates almost same range between x = 0.14–0.16 and y = 0.02–0.08. The colour difference observed in the CIE graph probably photophysical characteristics of different solvent environment with different polarities of molecular network structure. The emission shading tuning is more featured and obviously reacts to the pulling back of electrons of the substituents. These consequences are propelling for a significant comprehension of emission modification approaches and the new molecular engineering along with desirable scenery.

Conclusions

From the absorption and emission spectrum of C-466, noted that dye exhibit in all solvents shows a red-shift (bathochromic). These bathochromic shifts obtained with increasing polarity of solvent suggest that the transitions $\pi \rightarrow \pi^*$ involved. We also calculated the experimentally ground state dipole moments of C-466 from Bakshive, Kawski-Chamma methods. Excited state dipole moment are calculated by Kwaski–Chamma -Villet, Lippert – Mataga,

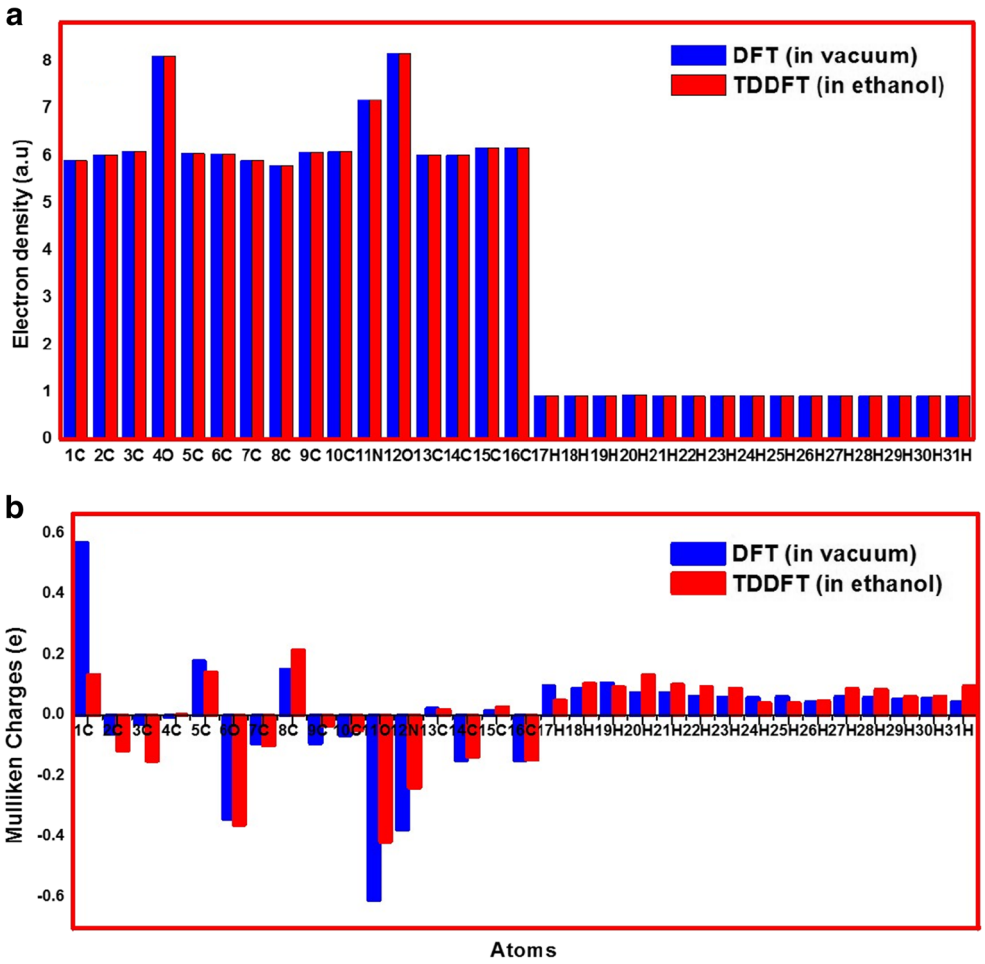

Fig. 16 Plots of (**a**) Electron density and (**b**) Mulliken atomic charge distributions for Coumarin-466

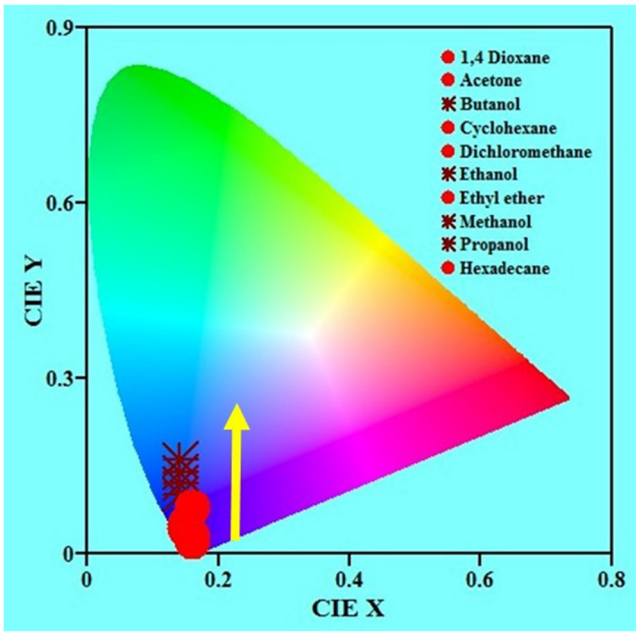

Fig. 17 CIE chromaticity plot for colour coordinates of Coumarin-466

Bakshieve's, E_T^N and McRae salvatochromic shift methods. From all methods, it is observed that μ_e* is higher than the μ_g. To obtain extra enlightenment of the molecular electronic properties for C-466, we examined hypothetical Ab initio quantum mechanical calculations which were executed in GAMESS performed time-dependent DFT (TD-DFT) using BECKE-1998 (exchange)/STO-6G basis set. The Highest Occupied Molecular Orbital and Lowest Unoccupied Molecular Orbital were calculated both in vacuum and solvent medium. The Solvent Accessible Surface (SAS) and Molecular Electrostatic Potential (MEP) were also analysed. Based on the optimized geometry, molecular orbital analysis for studied molecule, we observe from the energy gap of HOMO- LUMO is very small (0.2098 eV) which indicates π-π* transitions is easier, further probe molecule is more susceptibility and high chemical reactivity. Proposition comes to fruition are moving designed for additional ordered photophysical properties in different medium with different polarities of solvents can be for delineating to new luminescent test.

Acknowledgements The author Y.F. Nadaf thankful to Mohamed Zikriya, Promod A. G and Anilkumar Research Scholars from Bangalore University, Bangalore for assisting the preparation of this manuscript.

References

1. Bouckaert C, Serra S, Rondelet G, Dolusic E, Wouters J, Dogne JM, Frederick R, Pochet L (2016) Synthesis, evaluation and structure–activity relationship of new 3-carboxamide coumarins as FXIIa inhibitors. Eur J Med Chem 110:181–194
2. Sidarai AH, Desai VR, Hunagund SM, Basanagouda M, Kadadevarmath JS (2017) Study of Photophysical properties on newly synthesized Coumarin derivatives. J Fluoresc 27:2223–2229
3. Al-Kawkabani A, Makhloufi-Chebli M, Benosmane N, Boutemeur-Kheddis B, Hamdi M, Silva AMS (2017) Study of the novel fluorescent 4-methyl-9-(3-oxobutanoyl)-2H,8H-pyrano[2,3-f]chromene-2,8-dione derivative. Estimation of the ground- and excited-state dipole moments from a solvatochromic shift. J Mol Struct 1146:285–229
4. Kumari R, Varghese A, George L (2017) Estimation of ground-state and singlet excited-state dipole moments of substituted schiff bases containing oxazolidin-2-one moiety through solvatochromic methods. J Fluoresc 27:151–165
5. Renuka CG, Shivashankar K, Boregowda P, Bellad SS, Muregendrappa MV, Nadaf YF (2017) An experimental and computational study of 2-(3-Oxo- 3H-benzo[f] chromen-1-ylmethoxy)-benzoic acid methyl ester. J Sol Chem 46(8):1–22
6. Joshi S, Kumari S, Sarmah A, Sakhuja R, Debi D (2016) Pant, Solvatochromic shift and estimation of dipole moment of synthesized coumarin derivative: Application as sensor for fluorogenic recognition of Fe3 + and Cu2 + ions in aqueous solution. J Mol Liq 222:253–262
7. Durairaj A, Obadiah A, Ramanathan S, Johnson PM, Bella AP, Vasanthkumar S (2017) Synthesis, Characterization and Solvatochromic Studies Using the Solvent Polarity Parameter, ENT on 2-Chloro-3-Ethylamino-1,4-Naphthoquinone. 27:1505–1512
8. Benjamin LC, Dannielle GM, Rodrigo N, Samuel BP, Milan D, David DD, Sukrit M, Timothy SD, Naomi SG (2017) Tuning thermally activated delayed fluorescence emitter Photophysics through solvation in the solid state. ACS Energy Lett 2:1526–1533
9. Ghazy R, Azim SA, Shaheen M, El-Mekawey F (2004) Experimental studies on the determination of the dipole moments of some different laser dyes. Spectrochim Acta Part A Mol Biomol Spectrosc 60(1–2):187–191
10. Farley CM, Dibwe DF, Ueda JY, Hall EA, Awale S, Magolan J (2016) Evaluation of synthetic coumarins for antiausterity cytotoxicity against pancreatic cancers. Med Chem Lett 26:1471–1474
11. Gasbarri C, Angelini G (2017) Polarizability over dipolarity for the spectroscopic behavior of azobenzenes in room-temperature ionic liquids and organic solvents. J Mol Liq 229:185–188
12. Bhattacharya B, Samanta A (2007) Laser flash photolysis study of the aminophthalimide derivatives: elucidation of the nonradiative deactivation route. Chem Phys Lett 442(4–6):316–321
13. Reichardt C, Welton T (2010) Solvents and solvent effects in Org Chem Wiley-VCH Verlag GmbH and Co, Weinheim
14. Lakowicz JR (2006) Principles of fluorescence spectroscopy, Third edn. Plenum, New York
15. Stevens TS (1957) Chemistry of carbon compounds, IV A. Elsevier, Ed, By E.M. Rodd, Amsterdam
16. Lippert E (1957) Spektroskopische bistimmung des dipolmomentes aromatischer verbindugen im ersten angeregten singulettzustand. Z Electrochem 61:962–975
17. Bakshiev NG (1964) Universal intermolecular interactions and their effect on the position of the electronic spectra of molecules in two component solutions. Opt Specrtrosc 16:821–832
18. Chamma A, Viallet P (1970) Determination du moment dipolaire d'une molecule dans un etat excite singulet. Sci Paris Ser C 270: 1901–1904
19. McRae EG (1957) Theory of solvent effects on molecular electronic spectra frequency shifts. J Phys Chem 61:562–572
20. Edward JT (1956) Molecular volumes and parachor. Chem Ind 30: 774–777
21. Reichardt C (2005) Solvents and solvent effects in organic chemistry, VCH, Weinhwim;1988. Solvents and solvent effects in organic chemistry, VCH. In: New York
22. Kamlet MJ, Abboud JLM, Abraham MH, Taft RW (1983) Linear solvation energy relationships. A comprehensive collection of the solvatochromic parameters, π^*, α, and β, and some methods for simplifying the generalized solvatochromic equation. J Org Chem 48:2877–2887
23. Kamlet MJ, Abboud JLM, Taft RW (1977) The solvatochromic comparison method. 6. The π^* scale of solvent polarities. J Am Chem Soc 99:6027–6035
24. Pramanik S, Banerjee P, Sarkar A, Mukherjee A, Mahalanabis KK, Bhattacharya SC. Spectroscopic investigation of 3-pyrazolyl 2-pyrazoline derivative in homogeneous solvents. Spectrochim Acta Part A Mol Biomol Spectrosc 2008; 71:1327–1332
25. Homocianu M, Airinei A, Dorohoi DO (2011) Solvent effects on the electronic absorption and fluorescence spectra. J Adv Res 2:1–9
26. Sidir I, Gulseven Sidir Y, Kumalar M, Tasal E (2010) Ab initio Hartree-Fock and density functional theory investigations on the conformational stability, molecular structure and vibrational spectra of 7-acetoxy-6-(2,3-dibromopropyl)-4,8-dimethylcoumarin molecule. J Mol Struct 964:134–151
27. Sidir I, Sidir YG. Solvent effect on the absorption and fluorescence spectra of 7-acetoxy-6-(2,3-dibromopropyl)-4,8-dimethylcoumarin: determination of ground and excited state dipole moments. Spectrochim Acta Part A Mol Biomol Spectrosc 2013; 102: 286–296
28. Nadaf YF, Mulimani BG, Inamdar SR (2004) Ground and excited state dipole moments of some exalite UV laser dyes from solvatochromic method using solvent polarity parameters. J Mol Struct THEOCHEM 678:177–181
29. Raikar US, Renuka CG, Nadaf YF, Mulimani BG, Karguppikar AM, Soudagar MK. Solvent effects on the absorption and fluorescence spectra of coumarins 6 and 7 molecules: determination of ground and excited state dipole moment. Spectrochim Acta Part A Mol Biomol Spectrosc 2006; 65: 673–677
30. Masoud MS, Hagagg SS, Ali AE, Nasr NM (2012) Solvatochromic behaviour of the electronic absorption spectra of gallic acid and some of its azo derivatives. Spectrochim Acta Part A Mol Biomol Spectrosc 94:256–264
31. Singh M, Singh AK, Kumar R (2017) Investigation of charge-separation/change in dipole moment of 7-azaindole: quantitative measurement using solvatochromic shifts and computational approaches. J Mol Liq 231:39–44
32. Avadanei M, Cozan V, Avadanei O (2017) Solvatochromic properties of two related N -salicylidenanilines with dual fluorescence. J Mol Liq 227:76–86
33. Panigrahi M, Patel S, Mishra BK (2013) Solvatochromism of some hemicyanines. J Mol Liq 177:335–342
34. Kamlet MJ, Taft RW (1976) The solvatochromic comparison method. The α-scale of solvent hydrogen-bond donor (HBD) acidities. J Am Chem Soc 98:377–383

35. Schmidt MW, Baldridge KK, Boatz JA, Elbert ST, Gordon MS, Jensen JH, Koseki S, Matsunaga N, Nguyen KA, Su S, Windus TL, Dupuis M, Montgomery JA (1993) General atomic and molecular electronic structure system. J Comput Chem 14:1347–1363
36. Suvitha A, Periandy S, Gayathri P (2015) NBO, HOMO–LUMO, UV, NLO, NMR and vibrational analysis of veratrole using FT-IR, FT-Raman, FT-NMR spectra and HF–DFT computational methods. Spectrochim Acta Part A Mol Biomol Spectrosc 138:357–369
37. Chand S, Al-omary FAM, El-emam AA, Shukla VK, Prasad O, Sinha L (2015) Study on molecular structure, spectroscopic behavior, NBO, and NLO analysis of 3-methylbezothiazole-2-thione. Spectrochim Acta Part A Mol Biomol Spectrosc 146:129–141
38. Soliman SM, Hagar M, Ibid F, Sayed E, El Ashry H (2015) Experimental and theoretical spectroscopic studies, HOMO–LUMO, NBO analyses and thione – thiol tautomerism of a new hybrid of 1, 3, 4-oxadiazole-thione with quinazolin-4-one. Spectrochim Acta Part A Mol Biomol Spectrosc 145:270–279
39. Soliman SM, Albering J, Abu-youssef MAM (2015) Molecular structure, spectroscopic properties, NLO, HOMO–LUMO and NBO analyses of 6-hydroxy-3 (2H) –pyridazinone. Spectrochim Acta Part A Mol Biomol Spectrosc 136:1086–1098
40. Balachandran V, Lalitha S, Rajeswari S (2012) Density functional theory, comparative vibrational spectroscopic studies, NBO, HOMO–LUMO analyses and thermodynamic functions of N-(bromomethyl) phthalimide and N- (chloromethyl) phthalimide. Spectrochim Acta Part A Mol Biomol Spectrosc 91:146–157
41. Anton Georgiev, Anton Kostadinov, Deyan Ivanov, Deyan Dimov, Simeon Stoyanov Lian Nedelchev, Dimana Nazarova, Denitsa Yancheva. Synthesis, spectroscopic and TD-DFT quantum mechanical study of azo-azomethine dyes. A laser induced trans-cis-trans photoisomerization cycle. Spectrochim Acta Part A Mol Biomol Spectrosc 2018; 192:263–274
42. Toy M, Tanak H (2016) Molecular structure and vibrational and chemical shift assignments of 3 0-chloro-4-dimethylamino azobenzene by DFT calculations. Spectrochim Acta Part A Mol Biomol Spectrosc 152:530–536
43. Isa Sidir, Yadigar Gulseven Sidir. Solvatochromism and intramolecular hydrogen-bonding assisted dipole moment of phenyl 1-hydroxy-2-naphthoate in the ground and excited states. J Mol Liq 2016;221:972–985
44. Asiri AM, Sobahi TR, Osman OI, Khan SA (2017) Photophysical investigation of (D- p -a) DMHP dye : dipole moments, photochemical quantum yield and fluorescence quantum yield, by solvatochromic shift methods and DFT studies. J Mol Struct 1128:636–644
45. Sanmillan JL, Fernandez-Coello A, Fernandez-Conejero I, Plans G, Gabarros A (2017) Functional approach using intraoperative brain mapping and neurophysiological monitoring for the surgical treatment of brain metastases in the central region. J Neurosurg 126: 698–707
46. Thirumala PD, Crammond DJ, Loke YK, Cheng HL, Huang J, Balzer JR (2017) Diagnostic accuracy of motor evoked potentials to detect neurological deficit during idiopathic scoliosis correction: a systematic review. J Neurosurg Spine 26:374–383
47. Gowda V, Laitinen RS, Telkki VV, Larsson AC, Antzutkin ON, Lantto P (2016) DFT calculations in the assignment of solid-state NMR and crystal structure elucidation of a lanthanum(III) complex with dithiocarbamate and phenanthroline. Dalton Trans 45:19473–19484
48. Penghui Ren, Yuehua Zhang, Zhiwen Luo, Peng Song, Yuanzuo Li. Theoretical and experimental study on spectra, electronic structure and photoelectric properties of three nature dyes used for solar cells. J Mol Liq 2017; 247:193–206
49. Ayyanar Karuppasamy, Chandran Udhaya kumar, Muthiah Pillai Velayutham Pillai, Chennan Ramalingan. Synthesis, spectral, structural and DFT studies of novel dialkylfluorene decorated phenothiazine-3-carbaldehyde. J Mol Struct 2017; 1133:154–162
50. Isa Sıdır, Yadigar Gulseven Sidir, Halil Berber, Gulsen Turkoglu. Specific and non-specific interaction effect on the solvatochromism of some symmetric (2-hydroxybenzilydeamino) phenoxy Schiff base derivatives. J Mol Liq 2016; 215:691–703
51. Sidir I, Gulseven SY (2015) Estimation of ground and excited state dipole moments of oil red O by solvatochromic shift methods. Spectrochim Acta Part A Mol Biomol Spectrosc 135:560–567
52. Takjoo R, Centore R (2013) Synthesis, X-ray structure, spectroscopic properties and DFT studies of some dithiocarbazate complexes of nickel (II). J Mol Struct 1031:180–185
53. Nagarajan N, Velmurugan G, Prabhu G, Venuvanalingam P, Renganathan R (2014) A combined experimental and theoretical investigation of imidazole – carbazole fluorophores. J Lumin 147: 111–120
54. Pereira TM, Vitorio F, Amaral RC, Zanoni KPS, Iha NYM, Kummerle AE (2016) Microwave-assisted synthesis and photophysical studies of novel fluorescent N-acylhydrazone and semicarbazone-7-OH-coumarin dyes. New J Chem 40:8846–8854